Synthesis of Main-Chain Polyoxometalate-Containing Hybrid Polymers and Their Applications in Photovoltaic Cells

Meng Lu,[†] Baohan Xie,[†] Jeonghee Kang,[†] Fang-Chung Chen,[‡] Yang Yang,[‡] and Zhonghua Peng*,[†]

Department of Chemistry, University of Missouri−Kansas City, Kansas City, Missouri 64110, and Department of Materials Science and Engineering, University of California−Los Angeles, Los Angeles, California 90095

Received June 22, 2004. Revised Manuscript Received November 8, 2004

Hexamolybdate clusters have been embedded through covalent bonds into the main chain of poly(phenylene acetylene)s. These hybrid polymers were synthesized by palladium-catalyzed coupling reactions of a diiodo functionalized cluster with a diethynylbenzene derivative or a diethynyl functionalized cluster with a diiodobenzene derivative. These polymers are soluble in organic solvents such as *N*,*N*-dimethylformamide (DMF) and dimethyl sulfoxide (DMSO), and free-standing films can be spin-coated or cast from solutions. While hybrid monomer **2a** exhibits a sharp melting transition at 246 °C, polymers **5a** and **5b** show glass transitions at 125 and 102 °C, respectively. Cyclovoltammetry studies of the hybrid polymers revealed a reversible reduction wave at 1.19 V versus Ag/Ag^+, comparable to those of bifunctionalized imido derivatives of hexamolybdates. These polymers show intense absorption in the visible range but with little fluorescence emissions, indicating efficient fluorescence quenching of the embedded polyoxometalate (POM) cluster on the organic phenylene acetylene units. Simple single-layer photovoltaic (PV) cells with a device configuration of indium−tin oxide (ITO)/polymer/Ca have been fabricated and a power conversion efficiency of 0.15% has been obtained, which is significantly higher than PV cells fabricated with other conjugated polymers in the same device configuration. These results convincingly demonstrate the potential applications of POM-based organic−inorganic hybrids in molecular electronics and photonics.

Introduction

The past decade has witnessed significant advancement in the development of main-chain metal-containing polymers.[1] The motivation in exploring such polymers lies not only in the fundamental synthetic challenge[2] but also in the perspective of generating new materials with unique redox, electrical, optical, and magnetic properties.[3] The recent development of creative synthetic strategies and organometallic chemistry has allowed the synthesis of a variety of soluble high molecular weight organometallic main-chain polymers, including poly(metallocenes),[1f,4] poly(metal acetylides),[5] metal-containing polyynes,[6] and so forth. Most such polymers, however, contain discrete mononuclear or dinuclear metal centers. Efforts toward incorporating metal clusters in the main chain have had only limited success.[7]

Among various inorganic clusters, polyoxometalates (POMs) stand out not only in their structural diversity but also in the tunability of their many properties, ranging from molecular shape to solubility and from charge density to redox potentials.[8] In addition, the molecular nature of POM clusters

* Corresponding author: e-mail pengz@umkc.edu.
[†] University of Missouri-Kansas City.
[‡] University of California-Los Angeles.

(1) For reviews, see (a) *Inorganic and Metal-Containing Polymeric Materials*; Sheats, J. E., Caraher, C. E., Jr., Pittman, C. U., Jr., Zeldin, M., Surrel, B., Eds.; Plenum Press: New York, 1990. (b) Allcock, H. R. *Adv. Mater.* **1994**, *6*, 106−115. (c) Oriol, L.; Serrano, J. L. *Adv. Mater.* **1995**, *7*, 348−369. (d) Long, N. J. *Angew. Chem., Int. Ed. Engl.* **1995**, *34*, 21−38. (e) Barlow, S.; O'Hare, D. *Chem. Rev.* **1997**, *97*, 637−669. (f) Nguyen, P.; Gómez-Elipe, P.; Manners, I. *Chem. Rev.* **1999**, *99*, 1515−1548. (g) Archer, R. D. *Inorganic and Organometallic Polymers*: Wiley−VCH: New York, **2001**. (h) *Macromolecules Containing Metal & Metal-like Elements*; Abd-El-Aziz, A. S., Carraher, C. E., Jr., Pittman, C. U., Jr., Eds.; John Wiley and Sons: New York, 2004.

(2) (a) Nomura, R.; Watanabe, K.; Masuda, T. *Macromolecules* **2000**, *33*, 1936−1939. (b) Leung, A. C. W.; Chong, J. H.; Patrick, B. O.; MacLachlan, M. J. *Macromolecules* **2003**, *36*, 5051−5054. (c) Manners, I. *Angew. Chem., Int. Ed. Engl.* **1996**, *35*, 1602.

(3) (a) Wang, X.-S.; Arsenault, A.; Ozin, G. A.; Winnik, M. A.; Manners, I. *J. Am. Chem. Soc.* **2003**, *125* (42), 12686−12687 (a) Kulbaba, K.; Cheng, A.; Bartole, A.; Greenberg, S.; Resendes, R.; Coombs, N.; Safa-Sefat, A.; Greedan, J. E.; Stöver, H. D. H.; Ozin, G. A.; Manners, I. *J. Am. Chem. Soc.* **2002**, *124*, 12522. (b) Manners, I. *Science* **2001**, *294*, 1664. (c) Kingsborough, R. P.; Swager, T. M. *Prog. Inorg. Chem.* **1999**, *48*, 123. (d) Tsuda, A.; Osuka, A. *Science* **2001**, *293*, 79. (e) Screen, T. E. O.; Thorne, J. R. G.; Denning, R. G.; Bucknall, D. G.; Anderson, H. L. *J. Am. Chem. Soc.* **2002**, *124*, 9712−9713.

(4) See for example: (a) Manners, I. *Can. J. Chem.* **1998**, *76*, 371. (b) Resendes, R.; Nelson, J. M.; Fischer, A.; Jäkle, F.; Bartole, A.; Lough, A. J.; Manners, I. *J. Am. Chem. Soc.* **2001**, *123*, 2116−2126. (c) Mitzuta, T.; Imamura, Y.; Miyoshi, K. *J. Am. Chem. Soc.* **2003**, *125*, 2068−2069. (d) Papkov, V. S.; Gerasimov, M. V.; Dubovik, I. I.; Sharma, S.; Dementiev, V. V.; Pannell, K. H. *Macromolecules* **2000**, *33*, 7101−7115. (e) Bucaille, A.; Le Borgne, T.; Ephritikhine, M.; Daran, J. C. *Organometallics* **2000**, *19*, 4912.

(5) See for example: (a) Sonogashira, K.; Takahashi, S.; Hagihara, N. *Macromolecules* **1977**, *10*, 879. (b) Field, L. D.; Turnbull, A. J.; Turner, P. *J. Am. Chem. Soc.* **2002**, *124* (14), 3692−3702. (c) Fyfe, H. B.; Mlekuz, M.; Zargarian, D.; Taylor, N. J.; Marder, T. B. *J. Chem. Soc., Chem. Commun.* **1991**, 188. (d) Faulkner, C. W.; Ingham, S. L.; Khan, M. S.; Lewis J.; Long, N. J.; Raithby, P. R. J. *Organomet. Chem.* **1994**, *482*, 139. (e) Lavastre, O.; Even, M.; Dixneuf, P. H.; Pacreau, A.; Vairon, J. P. *Organometallics* **1996**, *15*, 1530. (f) Yamamoto, T.; Morikita, T.; Maruyama, T.; Kubota, K.; Katada, M. *Macromolecules* **1997**, *30*, 5390. (g) Irwin, M. J.; Vittal, J. J.; Puddephatt, R. J. *Organometallics* **1997**, *16*, 3541.

10.1021/cm049003r CCC: $30.25
Published on Web 12/29/2004

makes it possible to modify their structures at the molecular level in a rational and controlled version.[9] Indeed, great efforts have been devoted in developing hybrid polymers containing covalently linked POMs.[10] While numerous hybrid polymers with POM clusters incorporated in the side chains have been recorded and all of these polymers have electrically insulating non-π-conjugated backbones,[10] there has been no report, as far as we know, on main-chain POM-containing polymers. This is not surprising considering the difficulty in making pure difunctional organometallic species. We have previously reported a novel reaction that allows the selective synthesis of difunctionalized POM clusters.[11] We have also pointed out that the so-prepared difunctionalized clusters can be used as monomers for the synthesis of main-chain POM-containing hybrid polymers. We report herein the detailed synthesis of the first two POM-containing hybrid main-chain polymers and the studies of their electronic, optical, and electrochemical properties.

Results and Discussion

Synthesis of Monomers and Polymers. Scheme 1 shows the synthesis of bifunctionalized POM clusters with either two iodo or two ethynyl groups. As demonstrated previously,[11] by use of the tetrabutylammonium salt of an octamolybdate anion $[\alpha\text{-}Mo_8O_{26}]^{4-}$ as the starting cluster, bifunctionalized imido derivatives **2a** and **2b** are selectively synthesized in good yields. Both compounds are obtained as red crystals and are soluble in common organic solvents such as acetonitrile, methylene chloride, acetone, etc.

The structural characterization of **2a** has been reported previously.[11] The ^{1}H NMR spectrum of **2b**, shown in Figure 1, shows one singlet in the aromatic region. The signal corresponding to the ethynyl protons appears as a singlet at 3.39 ppm. The doublet at 1.27 ppm is attributed to the methyl

Scheme 1. Synthesis of Bifunctionalized Clusters

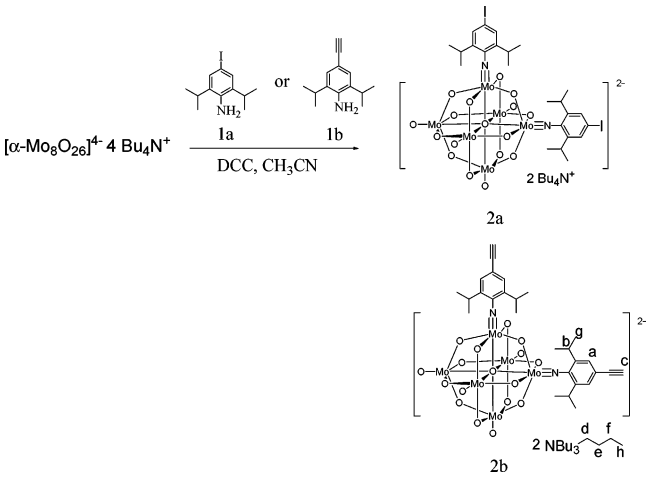

protons in the isopropyl substituents. The protons of the counterion give four signals at 0.96, 1.35, 1.60, and 3.10 ppm. The integration ratio of signals associated with protons in the functionalized cluster anion over those in the counterion, for example, protons g over h (see Scheme 1 for proton labeling), indicates a bifunctionalization in **2b**. Compared to the ^{1}H NMR spectrum of the corresponding monofunctionalized cluster, the aromatic signals in **2b** are slightly upfield-shifted (by ~0.3 ppm),[9c] which indicates a less electron-withdrawing nature of the Mo−N bond in **2b**, a result of better electron-donating power of imido ligands over oxo ligands. The ^{13}C NMR spectrum, which shows four aromatic carbon signals (110−130 ppm), two ethynyl carbons signals (83.4 and 80.1 ppm), and six alkyl carbon signals, is consistent with the structure. The elemental analysis (see Experimental Section) also confirmed the purity and the structure of compound **2b**.

The structure of **2b** was further studied by single-crystal X-ray diffraction. As shown in Figure 2, the molecular structure of **2b** confirmed the expected atom connectivity. Compound **2b** crystallizes in the triclinic space group *Pi*, as does compound **2a**.[11] The Mo−N bond distances in **2b** (1.74−1.75 Å) and **2a** (1.748 Å) are slightly longer than those found in their corresponding monosubstituted derivatives [1.729(5) and 1.733(6) Å, respectively], while the N−C distances (1.37−1.38 Å) are significantly shorter (1.52 Å),[9c,11] which indicates less triple-bond character in Mo−N bonds and more double-bond character in N−C bonds in the bifunctionalized clusters. This may be due to the fact that bifunctionalized clusters are more electron-rich, resulting in less ligand−metal pπ−dπ interaction. The cluster ions in the lattice of **2b** organize into dimers driven by hydrogen bonds between the rather acidic ethynyl proton of one cluster and the bridging oxygen atom of the other cluster.

The synthesis of the polymers is shown in Scheme 2. Both **2a** and **2b** can be used as monomers for the polymer synthesis. Polymer **5a** was synthesized by the Sonogashira coupling reaction of **2a** with **3** or **2b** with **4** in DMF at room temperature.[12,13] When excess organic base such as triethylamine was used, as usually happens in the Sonogashira coupling reaction, no polymer was obtained. While the coupling reaction did go through as compound **3** disappeared quickly, depolymerization occurred as some of the imido

(6) See for example: (a) Yam, V. W.-W. *Acc. Chem. Res.* **2002**, *35* (7), 555−563. (b) Wong, W.-Y.; Wong, C. K.; Lu, G. L.; Lee, A. W. M.; Cheah, K. W.; Shi, J. X. *Macromolecules* **2003**, *36* (4), 983−990. (c) Bunz, U. H. F. *Top. Curr. Chem.* **1999**, *201*, 131. (d) Xu, G. L.; Zou, G.; Ni, Y. H.; DeRosa, M. C.; Crutchley, R. J.; Ren, T. *J. Am. Chem. Soc.* **2003**, *125*, 10057. (e) Yao, H.; Sabat, M.; Grimes, R. N.; Zanello, P.; Fabrizi de Biani, F. *Organometallics* **2003**, *22* (13), 2581−2593. (f) Szafert, S.; Gladysz, J. A. *Chem. Rev.* **2003**, *103*, 4175.

(7) (a) Chan, W. Y.; Berenbaum, A.; Clendenning, S. B.; Lough, A. J.; Manners, I. *Organometallics* **2003**, *22*, 3796. (b) Berenbaum, A.; Lough, A. J.; Manners, I. *Organometallics* **2002**, *21*, 4415. (c) Schubert, U.; Volkel, T.; Moszner, N. *Chem. Mater.* **2001**, *13* (11), 3811. (d) Lucas, N. T.; Humphrey, M. G.; Rae, A. D.; *Macromolecules* **2001**, *34* (18), 6188.

(8) (a) Pope, M. T. *Heteropoly and Isopoly Oxometalates*: Springer-Verlag: New York, 1983. (b) Pope, M. T.; Müller, A. *Angew. Chem., Int. Ed. Engl.* **1991**, *30*, 34. (c) *Polyoxometalates: From Planotic Solids to Anti-Retroviral Activity*; Pope, M. T., Müller, A., Eds.; Kluwer Academic Publishers: Dordrecht, The Netherlands, 1994. (d) Hill, C. L. (guest editor) *Chem. Rev.* **1998**, *98*, 1.

(9) (a) Strong, J. B.; Yap, G. P. A.; Ostrander, R.; Liable-Sands, L. M.; Rheingold, A. L.; Thouvenot, R.; Gouzerh, P.; Maatta, E. A. *J. Am. Chem. Soc.* **2000**, *122*, 639−649. (b) Gouzerh, P.; Proust, A. *Chem. Rev.* **1901**, *1*, 77. (c) Wei, Y.; Xu, B.; Barnes, C. L.; Peng, Z. *J. Am. Chem. Soc.* **2001**, *123*, 4083.

(10) (a) Judeinstein, P. *Chem. Mater.* **1992**, *4*, 4. (b) Mayer, C. R.; Thouvenot, R.; Lalot, T. *Chem. Mater.* **2000**, *12*, 257. (c) Schroden, R. C.; Blanford, C. F.; Melde, B. J.; Johnson, B. J. S.; Stein, A. *Chem. Mater.* **2001**, *13*, 1074. (d) Johnson, B. J. S.; Stein, A. *Inorg. Chem.* **2001**, *40*, 801. (e) Moore, A. R.; Kwen, H.; Beatty, A. M.; Maatta, E. A. *Chem. Commun.* **2000**, 1793.

(11) Xu, L.; Lu, M.; Xu, B.; Wei, Y.; Peng, Z.; Powell, D. R. *Angew. Chem., Int. Ed.* **2002**, *41* (21), 4129.

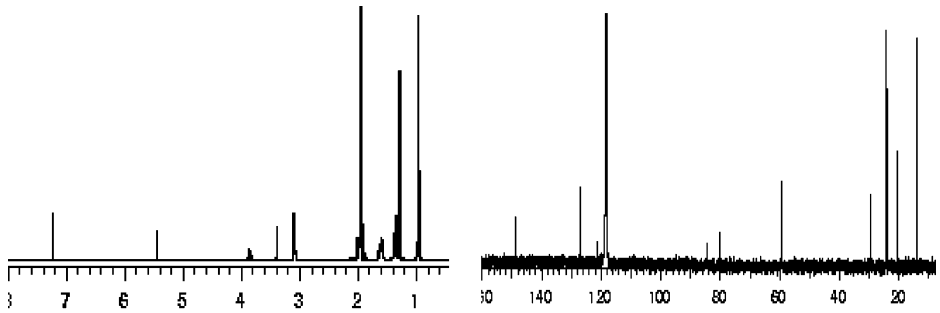

Figure 1. ^{1}H NMR and ^{13}C NMR spectra of **2b** in acetonitrile.

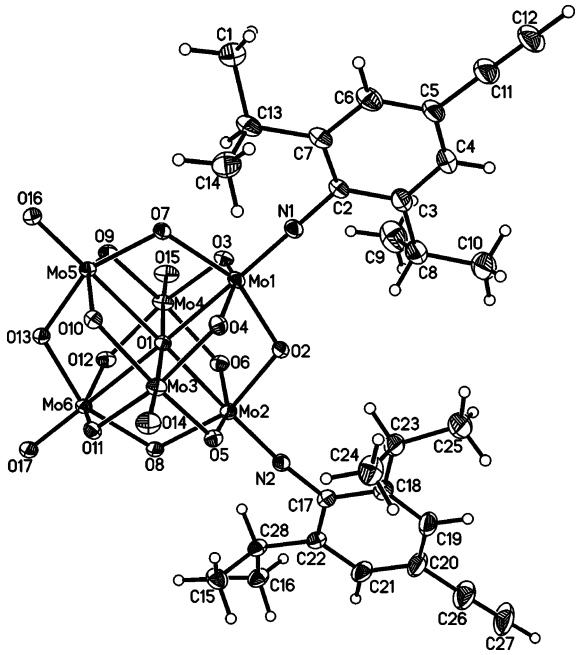

Figure 2. Anion structure of **2b**. The displacement ellipsoids were drawn at the 50% probability level. Selected bond lengths (angstroms) and bond angles (degrees): Mo1−N1 1.743(3), Mo1−O1 2.2173(19), Mo2−N2 1.750(3), Mo2−O1 2.2239(19), Mo3−O14 1.698(2), Mo3−O1 2.3558(19), Mo4−O15 1.693(2), Mo4−O1 2.3518(19), Mo5−O16 1.687(2), Mo5−O1 2.3828(19), Mo6−O16 1.685(2), Mo6−O1 2.3689(19), N1−C2 1.378-(4), N2−C17 1.376(4); Mo1−N1−C2 175.0(3), Mo2−N2−C17 173.6(2).

bonds (Mo−N bonds) were broken, especially with prolonged reaction time.[13] It appears that the Mo−N bond is not very stable in the presence of excess triethylamine. Lowering the amount of triethylamine, however, significantly decreases the polymerization rate. Fortunately, the polymerization can be accelerated by adding excess K_2CO_3. Thus, with 1 equiv of triethylamine and excess K_2CO_3, polymer **5a** was obtained after 24 h of reaction. The resulting polymer is a dark red powder. Copolymer **5b**, with lower cluster loading in the polymer backbone, was synthesized by a similar coupling reaction of **2a** with compounds **3** and **4**. The molar ratio of **2a**:**3**:**4** is 1:2:1. Both polymers **5a** and **5b** exhibit excellent solubility in DMF and DMSO.

In polymers **5a** and **5b**, the covalently embedded clusters are linked by a rigid conducting oligo(phenylene ethynylene) bridge. The repeating structural unit, particularly of polymer **5a**, resembles the structure of our previously reported cluster

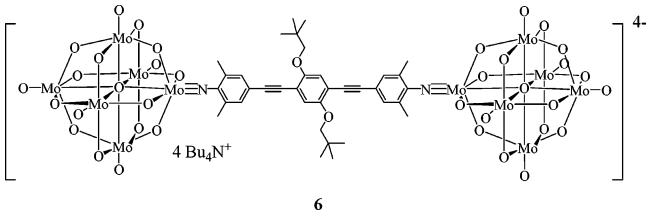

6

Figure 3. Structure of hybrid dumbbell **6**.

Scheme 2. Synthesis of Hybrid Polymers 5a and 5b

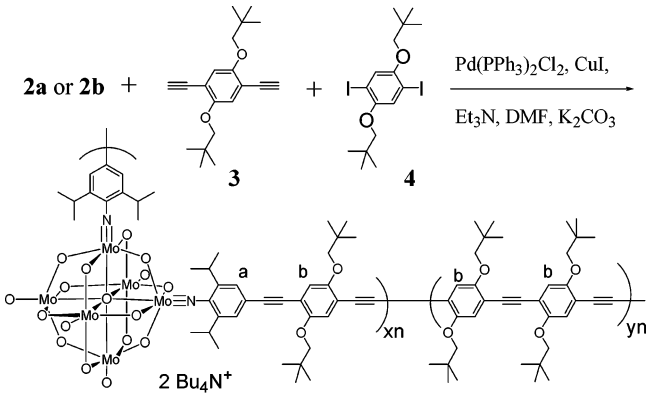

Polymer **5a**: x = 1, y = 0
Polymer **5b**: x = 1, y = 1

dumbbell **6** (Figure 3).[14] Indeed, the ^{1}H NMR spectra of polymer **5a** and dumbbell **6**, shown in Figure 4, are quite similar. Both spectra show two signals in the aromatic region with an integration ratio close to 2:1, consistent with their structures. Peaks corresponding to protons in the counterion (3.10, 1.60, 1.35, and 0.96 ppm) appear at nearly identical chemical shifts in both spectra. Notice that the ^{1}H NMR spectrum of **5a** has two additional peaks at 3.81 and 1.25 ppm, while the spectrum of **6** has one additional signal at 2.59 ppm. This is due to the fact that the cluster-bonding phenyl rings in **5a** have two isopropyl substituents, while those in **6** have two methyl substituents. Polymer **5a** also shows a very small peak at 7.47 ppm that was identified as the end-group protons associated with the aromatic terminus. The integration ratio of the peak at 7.47 ppm vs that at 7.32 ppm is 1:18. Assuming both ends of the polymer are capped by the iodo end group (as no acetylene proton signal is observed in the NMR), this integration ratio gives the number of repeating units at 18.

The ^{1}H NMR spectrum of copolymer **5b** is shown in Figure 5. The aromatic protons in the cluster-binding phenyl

(12) Sonogashira, K.; Tohda, Y.; Hagihara, N. *Tetrahedron Lett.* **1975**, 4467
(13) Xu, B.; Wei, Y.; Barnes, C. L.; Peng, Z. *Angew. Chem., Int. Ed.* **2001**, *40* (12), 2290.
(14) Lu, M.; Wei, Y.; Xu, B.; Cheung, C. F.-C.; Peng, Z.; Powell, D. *Angew. Chem., Int. Ed.* **2002**, *41* (9), 1566.

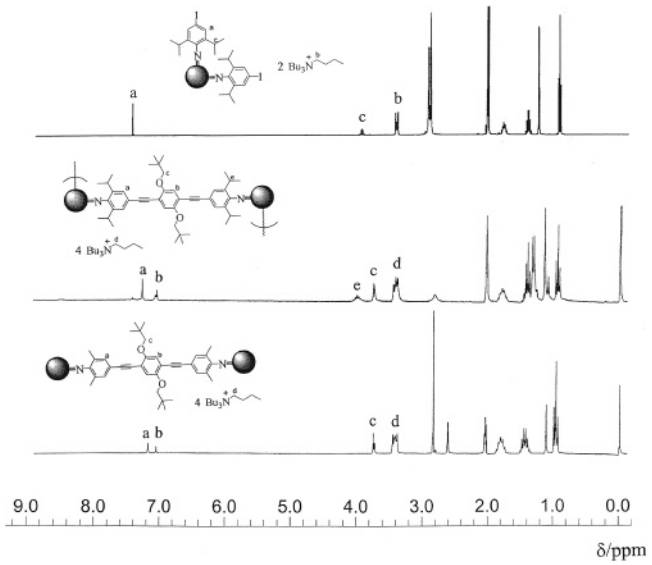

Figure 4. ^{1}H NMR spectra of monomer **2a**, polymer **5a**, and dumbbell **6** in acetone-d_6.

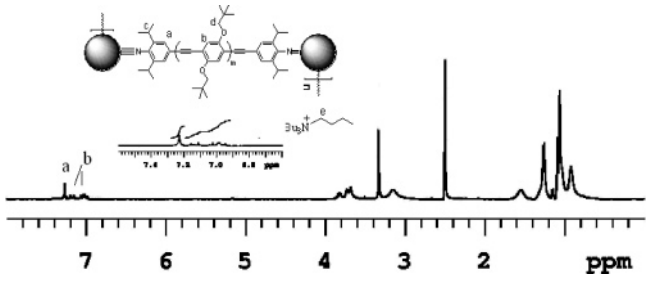

Figure 5. ^{1}H NMR spectrum of polymer **5b** in DMSO.

rings (proton a; see Scheme **2** for proton labeling) appear as a relatively sharp signal at 7.27 ppm. Protons in the middle phenyl rings ortho to the alkoxy substituents (protons b) give multiple broad peaks from 6.99 to 7.20 ppm, unlike those in polymer **5a** where they appear as only one broad peak, indicating varied bridge lengths between embedded clusters in polymer **5b**. On the basis of the integration ratio of 1:1.5 of signal a over signals b combined, an average bridge length of five phenyl rings and four triple bonds can be deduced, which is consistent with the monomer feeding ratios. The end-group proton signals seen in the spectrum of **5a** were not observed in the ^{1}H NMR spectrum of **5b**. Elemental analysis gave both C and Mo contents within 2% of theoretical values. These results point to higher degrees of polymerization for polymer **5b** than polymer **5a**.

The Fourier transform infrared (FTIR) spectra of polymers **5a** and **5b** both show two strong, broad bands at 782 and 940 cm^{-1}, which are attributed to ν(Mo−O−Mo) and ν(Mo═O), respectively. A shoulder peak at 967 cm^{-1} can be identified that corresponds to ν(Mo═N). The ν(C≡C) band appears at 2194 cm^{-1}, typical of ArC≡CAr triple bonds.

Molecular Weights. Besides end-group analysis, other techniques such as viscometry, gel-permeation chromatography (GPC), and light scattering measurements have been applied to evaluate the molecular weights of the hybrid polymers. The GPC measurements, which were carried out at 30 °C on a Styrogel 4E column with DMF as the eluent

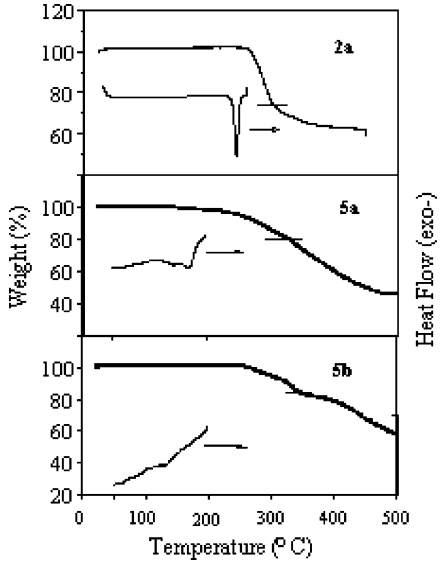

Figure 6. DSC and TGA thermograms of hybrids **2a**, **5a**, and **5b** under nitrogen.

and polystyrenes as the standards, give weight-average molecular weights of 161 000 and 162 000 for **5a** and **5b**, respectively. It is noted that the separation of hybrid polymers in GPC columns is very poor as exceedingly narrow molecular weight distributions (<1.05) for both **5a** and **5b** were obtained. While the molecular weights based on GPC (relative to polystyrene standards, which are clearly not good standards for the rigid polymers) may be questionable, light scattering analysis, performed on a Dawn EOS system from Wyatt Technologies with an Optilab rEX DRI detector, gives an average molecular weight of 91 kg/mol, indicating polymers are indeed obtained. The intrinsic viscosity for polymer **5a**, measured on an Ubbelohde capillary viscometer at 30 °C, is 0.2 dL/g. It should be noted that the polyelectrolyte nature, the rigid and yet zigzag backbone characteristics, and the possible peculiar aggregation behavior of the hybrid polymers may render the applicability of these techniques questionable. Nonetheless, it is reasonable to claim that hybrid polymers are indeed produced.

Thermal Properties. While numerous imido derivatives of hexamolybdates have been reported, there has been no report as far as we know on their thermal properties. We have studied the thermal properties of hybrid **2a** and polymers **5a** and **5b** by differential scanning calorimetry (DSC) and thermogravimetric analysis (TGA). As shown in Figure 6, monomer **2a** exhibits a sharp melting transition at around 240 °C, while polymers **5a** and **5b** show glass transitions at 125 and 102 °C, respectively. All of these hybrids are thermally stable up to 250 °C. The decomposition of these hybrids appears to be separated into two stages, which is particularly clear for polymers **5a** and **5b**. The weight loss associated with the first stage is around 26%, 21%, and 18%, respectively, for **2a**, **5a**, and **5b**, which fits reasonably well with the weight percentage of counterions in their respective compositions (25%, 24%, and 19%). It is likely that counterions are lost first, followed by the cluster-bond organic segments.

Electronic Properties. Figure 7 shows the UV/vis absorption spectra of compounds **2a** and **2b** and polymers **5a** and

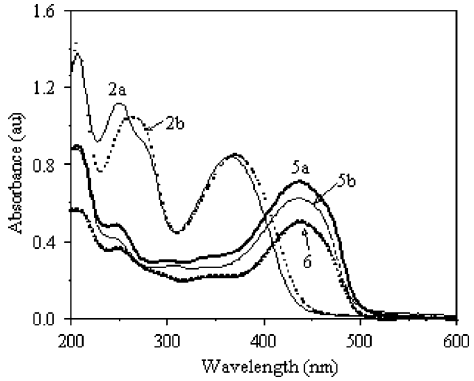

Figure 7. UV/Vis absorption spectra of **2a**, **2b**, **5a**, **5b**, and **6** in acetonitrile.

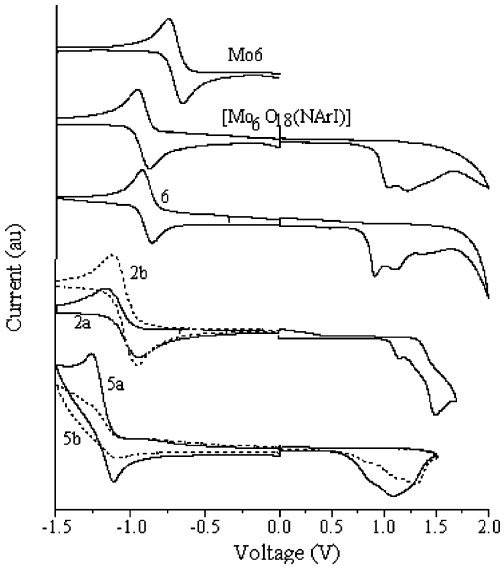

Figure 8. Cyclic voltammograms of the hexamolybdate, its mono- and bifunctionalized derivatives, the dumbbell **6**, and the hybrid polymers.

5b, as well as dumbbell **6**. The absorption spectra of polymers **5a** and **5b** are again remarkably similar to that of dumbbell **6**. All of them have a broad absorption peak at 438 nm in the visible range, which is significantly bathochromically shifted from those of **2a** and **2b**. The lowest energy electronic transitions are attributed to the ligand-to-metal charge transfer (LMCT) transition involving the Mo−N π bonds. The contribution of the $\pi-\pi^*$ transition associated with the organic conjugated bridge cannot be ruled out, however. Note that dialkoxysubstituted poly(phenylene ethynylenes), for example, polymer **5c** ($x = 0$, $y = 1$ in Scheme **2**), have absorption maxima around 450 nm.[15] Fluorescence studies show that both polymers **5a** and **5b** exhibit no fluorescence at room temperature under excitation from 200 to 500 nm, while polymer **5c** is strongly fluorescent. Apparently, the nonemissive LMCT excited-state quenches $\pi-\pi^*$ transition states.

Electrochemistry. Figure 8 shows the cyclovoltammograms of the parent hexamolybdate cluster, the monofunctionalized cluster $[Mo_6O_{18}(N(^iPr)_2C_6H_3I]$, the bifunctionalized monomers **2a** and **2b**, dumbbell **6**, and the hybrid polymers. During the cathodic scan, all hybrids exhibit one reversible reduction wave, although the two polymers show less

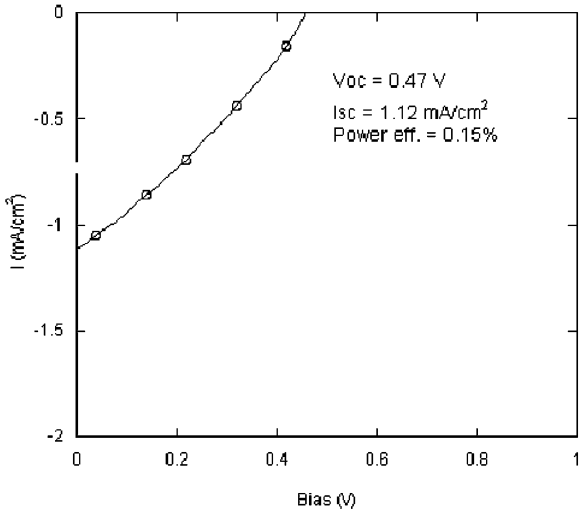

Figure 9. Current density vs voltage for an ITO/polymer **5a**/Ca device.

reversibility. Note that the cyclic voltammograms of polymers were measured on polymer films while those of small compounds (**2a**, **2b**, and **6**) were based on solutions. As observed previously, the reduction becomes progressively more difficult from the parent cluster to the monofunctionalized cluster and to the diimido derivatives.[9a] The reduction potential of dumbbell **6** is very close to that of the monofunctionalized cluster, while polymers **5a** and **5b** show similar reduction potentials to those of diimido-functionalized monomers. Clearly, the Mo−N imido bonds survived the polymerization and purification processes. It is noted that the reduction potentials of the hybrids depend mainly on the number of imido ligands, while showing little dependence on the π-conjugation length of the organic segments. Clearly, the reduction process is associated with the clusters. On the other hand, during the anodic scan, all hybrids exhibit irreversible oxidation waves that show strong dependence on the organic segments. The oxidation potentials decrease from **2a** to **6** and to hybrid polymers, reflecting continuously increased π-conjugation. The oxidation processes are thus attributed to the removal of π-electrons from the organic conjugated systems.

Photovoltaic Devices. Photovoltaic devices with a thin layer of polymer **5a** sandwiched between a transparent anode (indium−tin oxide, ITO) and a metal cathode have been fabricated. Figure 9 shows the current−voltage ($I-V$) of the device under 100 mW/cm^2 illumination (AM1.5G). The open-circuit voltage (V_{oc}) and short-circuit current (I_{sc}) are 0.47 V and 1.12 mA/cm^2, respectively. The filling factor is 0.29. The calculated power conversion efficiency is 0.15%. The I_{sc} and power conversion efficiency are more than 1 order of magnitude higher than those of a typical single-layer polymer device with similar device structures, such as the one with poly[2-methoxy-5-(2′-ethylhexyloxy)-1,4-phenylvinylene] (MEH-PPV) as the active layer.[16]

For a typical polymer, the absorbed photons mainly create excitons, which have strong binding energy.[17] Because the excitons usually decay geminately (either radiatively with photoluminescence or nonradiatively), the number of free

(15) Bunz, U. H. F. *Chem. Rev.* **2000**, *100* (4), 1605.

(16) Yu, G.; Zhang, C.; Heeger, A. J. *Appl. Phys. Lett.* **1994**, *64*, 1540.

charge carriers in the device is usually very small, which limits the photocurrent and device efficiency.[18] Consequently, efficient polymer photovoltaic devices usually require the addition of strong electron acceptors, such as C_{60}, to promote charge separation.[19] The much higher I_{sc} and power conversion efficiency achieved with hybrid polymer **5a** suggest that photoinduced charge separation in such hybrid polymers may be rather efficient, which is also supported by the absence of photoluminescence. It is realized, though, that the PV cell performance of such hybrid polymers pales in comparison with the best polymer-based devices reported so far.[20] The power conversion efficiency may be limited by the poor charge-transporting properties of these polymers since they contain only limited π-extended conjugated segments. Conjugated polymers with POMs as side-chain pendants may be better candidates for photovoltaic applications. Efforts in making such hybrid polymers are in progress.

Conclusions

Conjugated polymers with hexamolybdate clusters embedded in the main chain through covalent bonds have been prepared for the first time through Pd-catalyzed coupling reactions. The structures of the hybrid polymers were confirmed by ^{1}H NMR, FTIR, and elemental analysis. Although the molecular weights of these polymers are moderate, good quality free-standing films can be cast from solutions. While hybrid monomer **2a** exhibits a sharp melting transition at 246 °C, polymers **5a** and **5b** show glass transitions at 125 and 102 °C, respectively. Cyclic voltammetry studies show that these hybrid polymers exhibit a reversible reduction wave at −1.19 V, similar to those of diimido derivatives of hexamolybdates. These polymers show intense absorption in the visible range but with no fluorescence emissions, indicating efficient fluorescence quenching of the embedded POM cluster on the organic phenylene acetylene units. Preliminary photovoltaic studies have shown that these polymers can be fabricated as single-layer photovoltaic cells showing respectable power conversion efficiencies.

Experimental Section

The synthesis of compound **2a** has been reported previously. All of the other chemicals were purchased from either Acros or Aldrich and were used as received unless otherwise stated. The ^{1}H NMR spectra were collected on a Varian 400 MHz FT NMR spectrometer. Thermal analyses were performed on Shimadzu DSC-50 and TGA-60. GPC measurements were performed at 30 °C on a Waters setup (a Waters 210 pump, a Waters R401 differential refractometer, and a Styragel 4E column) with DMF as the eluent. The calibration curve was determined by use of five polystyrene standards from 800 to 90 000. Light scattering analysis was carried out on a Dawn EOS system with an Optilab rEX DRI detector from Wyatt Technologies. A Hewlett-Packard 8452A diode-array spectrophotometer was used to record the UV/vis absorption spectra. Photoluminescence properties were measured on a Shimadzu RF-5301PC spectrofluorophotometer. Cyclic voltammetry (CV) studies were carried out in acetonitrile at room temperature under the protection of nitrogen by use of a BAS Epsilon EC electrochemical station employing a 1 mm^2 Pt disk as the working electrode, Ag/Ag^+ electrode (0.01 M $AgNO_3$) as the reference electrode, and a Pt wire as the counterelectrode. $[Bu_4N]PF_6$ was the supporting electrolyte, and the scan rate was 200 mV s^{-1}. Under these conditions, the $[Cp_2Fe]/[Cp_2Fe]^+$ couple was observed at $E_{1/2} = 100$ mV. For compounds **2a**, **2b**, and **6**, the measurements were done in their acetonitrile solutions. For polymers **5a** and **5b**, a thin polymer film was first cast onto the Pt disk working electrode and the voltammograms were recorded in acetonitrile.

The fabrication procedures of the polymer photovoltaic cells started with cleaning the ITO glass substrate by ultrasonic cleaner with sequential treatments of detergent, deionized water, acetone, and 2-propanol. The cleaned ITO surface was then modified by a spin-coating of 80 nm PEDOT/PSS (Baytron P VP Al 4083). A polymer **5a** solution was then spin-coated from DMF on the prepared substrates. The thickness of the polymer film is around 0.1 μm. The bilayer cathodes of devices, consisting of 500 Å of Ca and 1000 Å of Al, were thermally deposited on the top of films at $\sim 10^{-6}$ Torr. The device active area is 0.12 cm^2. The $I-V$ curves were obtained by a Keithley 2400 source-measure unit. The photocurrent was measured under illumination from a solar simulator [Thermo-Oriel 150W solar simulator (AM1.5G)]. All devices were fabricated and tested in a nitrogen environment.

Compound 2b. A mixture of $(NBu_4)_4[Mo_8O_{26}]$ (4.31 g, 2.0 mmol), 2,6-diisopropyl-4-ethynylaniline (1.01 g, 4.1 mmol), and dicyclohexylcarbodiimide (1.03 g, 4.1 mmol) in acetonitrile (10 mL) was refluxed for 7 h and then cooled to room temperature. The precipitates were separated by filtration and the filtrate was concentrated to 5 mL. Orange-red crystals, formed from the concentrated solution while setting at room temperature overnight, were filtered and dried in a vacuum. Further purification was done by column chromatography [silica gel (250−400 mesh)], with $CH_3CN/CH_2Cl_2 = 1{:}4$ as the eluent to yield the title compound as orange crystals (3.0 g, yield 87%). ^{1}H NMR (CD_3CN, δ) 7.24 (s, 4 H, aryl H), 3.85 (m, 4 H, $CHMe_2$), 3.39 (s, 2 H, CCH), 3.10 (m, 16 H, CH_2 in Bu), 1.60 (m, 16 H, CH_2 in Bu), 1.35 (m, 16 H, CH_2 in Bu), 1.27 (d, 24 H, CH_3 in iso-Pr), 0.96 (t, 24 H, CH_3 in Bu); ^{13}C NMR (CD_3CN, δ) 148.9, 126.9, 121.3, 83.4, 80.1, 59.3 (t, $J_{N-C} = 5.0$ Hz), 29.3, 24.3, 24.0, 20.3, 13.8. Anal. Calcd for $C_{60}H_{106}Mo_6N_4O_{17}$: C, 41.63; H, 6.17; N, 3.24. Found: C, 41.26; H, 6.15; N, 3.30. Orange prism-shaped single crystals of **2b** were grown by slow diffusion of diethyl ether into an acetonitrile solution of **2b**. Summary of crystal structure data for **2b**: $C_{60}H_{106}Mo_6N_4O_{17}$, $M_r = 1731.13$, triclinic, *Pi*, $a = 12.647(2)$ Å, $b = 12.769(2)$ Å, $c = 22.883(4)$ Å, $\alpha = 89.166(4)°$, $\beta = 78.266(4)°$, $\gamma = 80.941(4)°$, $V = 3572.4(10)$ Å^3, $Z = 2$, $Z' = 1$, $T = 100(2)$ K, 22 776 reflections measured, 13 547 unique ($R_{int} = 0.0146$), $R1 = 0.0342$, $wR2 = 0.0919$, GOF 1.017. CCDC-201038 contains the supplementary crystallographic data for this paper. These data can be obtained free of charge via www.ccdc.cam.ac.uk/conts/retrieving.html [or from the Cambridge Crystallographic Data Center, 12 Union Road, Cambridge CB21EZ, U.K.; fax (+44)1223-336-033 or deposit@

(17) Pope, M.; Swenberg, C. E. *Electronic Processes in Organic Crystals and Polymers*; Oxford University Press: Oxford, U.K., 1999.
(18) Brabec, C. J.; Sariciftci, N. S.; Hummelen, J. C. *Adv. Mater*. **2001**, *11*, 15−26.
(19) (a) Ramos, A. M.; Rispens, M. T.; van Duren, J. K. J.; Hummelen, J. C.; Janssen, R. A. J. *J. Am. Chem. Soc.* **2001**, *123*, 6714. (b) Brabec, C. J.; Cravino, A.; Zerza, G.; Sariciftci, N. S.; Kiebooms, R.; Vanderzande, D.; Hummelen, J. C. *J. Phys. Chem. B* **2001**, *105*, 1528. (c) Yang, X.; van Duren, J. K. J.; Janssen, R. A. J.; Michels, M. A. J.; Loos, J. *Macromolecules* **2004**, *37*, 2151.
(20) (a) Huynh, W. U.; Dittmer, J. J.; Alivisatos, A. P. *Science* **2002**, *295*, 2425. (b) Peumans, P.; Uchida, S.; Forrest, S. R. *Nature* **2003**, *425*, 158. (c) Liu, J.; Tanaka, T.; Sivula, K.; Alivisatos, A. P.; Frechet, J. M. J. *J. Am. Chem. Soc.* **2004**, ASAP, DOI 10.1021.

ccdc.cam.ac.uk].

Polymer 5a. The mixture of compound **3** (0.0597 g, 0.2 mmol), compound **2a** (0.3870 g, 0.2 mmol), bis(triphenylphosphine)-palladium(II) chloride (0.006 g, 0.008 mmol), copper(I) iodide (0.003 g, 0.016 mmol), triethylamine (0.04 g, 0.4 mmol), potassium carbonate (0.55 g, 4 mmol), and DMF (3 mL) was stirred at room temperature overnight. The reaction mixture was then filtered to remove the potassium carbonate. The filtrate was poured into methanol (30 mL) and the polymer precipitated as a dark red solid. The polymer was collected by filtration. It was further purified by redissolving in DMF and then reprecipitating from methanol. The polymer was collected by filtration and dried under vacuum (yield 78%). ^{1}H NMR (400 MHz, acetone-d_6, 25 °C) δ 7.32 (br, ArH, 4 H), 7.10 (br, ArH, 2 H), 4.04 (br m, −CH, 4 H), 3.79 (br, OCH_2, 4 H), 3.45 (t, J = 6.25 Hz, NCH_2, 16 H), 1.81 (br, CH_2, 16 H), 1.44 (m, CH_2, 16 H), 1.34 [d, J = 7.50 Hz, CH_3 of (Ar-)$CHMe_2$, 24 H], 1.17 (s, 18 H, CH_3 in alkoxy chains), 0.97 (t, J = 7.37 Hz, CH_3, 24 H). FT-IR data (cm^{-1}) 2960 (s), 2871 (s), 2194 (m), 1624 (m), 1589 (m), 1499 (m), 1466 (w), 1411 (m), 1395 (m), 1363 (m), 1273 (m), 1219 (m), 1047 (m), 1019 (m), 966 (s, sh), 946 (s), 882 (m), 778 (s). Anal. Calcd for the repeat unit $C_{76}H_{128}N_4O_{17}Mo_6$ (%): C, 46.91; H, 6.63; N, 2.88; Mo, 29.59. Found: C, 44.24; H, 5.86; N, 2.89; Mo, 27.89. Polymer **5a** was also synthesized by the coupling reaction of **2b** with monomer **4** under the same reaction conditions and workup procedures. The resulting polymer exhibits slightly lower molecular weights.

Polymer 5b. The mixture of compound **3** (0.1194 g, 0.4 mmol), compound **2a** (0.3870 g, 0.2 mmol), compound **4** (0.1004 g, 0.2 mmol), bis(triphenylphosphine)palladium(II) chloride (0.012 g, 0.016 mmol), copper(I) iodide (0.006 g, 0.032 mmol), triethylamine (0.08 g, 0.8 mmol), potassium carbonate (1.1 g, 8 mmol), and DMF (3 mL) was reacted to yield the copolymer (yield 77%). The workup procedure is similar to that of **5a**. ^{1}H NMR (400 MHz, DMSO-d_6, 25 °C) δ 7.27(br, ArH, 4 H), 7.20−6.99 (br m, ArH, 6 H), 3.84 (br m, −CH, 4 H), 3.74−3.68 (br m, OCH_2, 12 H), 3.15 (br, NCH_2, 16 H), 1.55 (br, CH_2, 16 H), 1.26 [m, $NCH_2CH_2\mathit{CH_2}$ and CH_3 of (Ar-)$CHMe_2$, 40 H], 1.06 (br m, 54 H, CH_3 in alkoxy chains), 0.92 (br, CH_3, 24 H). FT-IR data (cm^{-1}) 2959 (s), 2871 (s), 2196 (m), 1625 (w), 1589 (m), 1499 (m), 1475 (s), 1420 (m), 1397 (s), 1365 (m), 1273 (m), 1218 (s), 1048 (m), 1019 (m), 966 (m, sh), 946 (s), 897 (s), 884 (s), 841 (s), 779 (s). Anal. Calcd for the repeat unit $C_{112}H_{176}N_4O_{23}Mo_6$ (%): C, 53.33; H, 7.03; N, 2.22; Mo, 22.82. Found: C, 51.96; H, 6.65; N, 2.19; Mo, 20.19.

Acknowledgment. We thank Dr. Douglas R. Powell at the University of Kansas for the X-ray structure determination and Dr. Michelle H. Chen at Wyatt Technologies for the light scattering measurements. This work is supported by the National Science Foundation (DMR 0134032) and the Office of Naval Research.

CM049003R